Correlation Mapping for Visualizing Propagation of Pulsatile CSF Motion in Intracranial Space Based on Magnetic Resonance Phase Contrast Velocity Images: Preliminary Results

Satoshi Yatsushiro[1]-*IEEE Member*, Akihiro Hirayama[2], Mitsunori Matsumae[2], Nao Kajiwara[3], Afnizanfaizal Abdullah[4], Non-member, Kagayaki Kuroda[1], *IEEE Member*

[1] Course of Information Science and Engineering, Graduate School of Engineering, Tokai University, 4-1-1 Kitakaname, Hiratsuka, Kanagawa 259-1292, Japan

[2] Department of Neurosurgery, Tokai University School of Medicine, 143 Shimokasuya, Isehara, Kanagawa 259-1193, Japan

[3] Department of Radiology, Tokai University Hospital, 143 Shimokasuya, Isehara, Kanagawa 259-1193, Japan

[4] Faculty of Computer Science and Information Systems, Universiti Teknologi Malaysia, Johor, Malaysia

***Abstract*—Correlation time mapping based on magnetic resonance (MR) velocimetry has been applied to pulsatile cerebrospinal fluid (CSF) motion to visualize the pressure transmission between CSF at different locations and/or between CSF and arterial blood flow. Healthy volunteer experiments demonstrated that the technique exhibited transmitting pulsatile CSF motion from CSF space in the vicinity of blood vessels with short delay and relatively high correlation coefficients. Patient and healthy volunteer experiments indicated that the properties of CSF motion were different from the healthy volunteers. Resultant images in healthy volunteers implied that there were slight individual difference in the CSF driving source locations. Clinical interpretation for these preliminary results is required to apply the present technique for classifying status of hydrocephalus.**

I. Introduction

Principal driving forces of CSF flow dynamics has not been understood completely [1]. Yamada et al. have reported that travel of CSF can be visualized by a spin labeling technique called time-Spatial Labeling Inversion Pulse (Time-SLIP) [2]. Some literatures related to four-dimensional phase contrast (4D-PC) analyses were being published recently [3-5], because the technique is useful to visualize spatiotemporal CSF flow dynamics. The most significant difference between this technique and the Time-SLIP technique is that this technique visualizes the propagation of the CSF motion not the travel of proton spins: this feature allows to visualize such a propagation even if the CSF space is separated by a thin membrane-like structure such as liliequist membrane (LM) and an arachnoid cyst wall [6].

However, 4D-PC cine images are difficult to be used for understanding particular flow dynamics. Therefore a quantitative analysis technique to "freeze" the dynamics was required, and thus a novel technique called correlation time mapping was proposed [7-8]. This technique consists of two parts, the correlation time mapping and correlation coefficient mapping. The former technique presented delay time of propagation of the pulsatile CSF motion from a particular point in CSF space to the other. As CSF is an uncompressed liquid, the presence of propagation delay indicates the presence of compliance in the CSF space. Moreover the correlation coefficient mapping will tell us the similarity of the spatiotemporal CSF velocity patterns: The maps will indicate the presence of compliance and resistance in the CSF pathway. Although a similar analyzing technique for analyzing the blood flow of middle cerebral artery in brain has been reported previously based on contrast-enhanced X-ray CT images [9], to our best knowledge, the present study is the first to observe the CSF velocity fields taken by non-contrast enhanced MR images. When the reference point is placed in blood flow and the points in CSF is observed, this technique will give information about the pressure propagation from blood flow to CSF motion. However, the property of the correlation mapping in evaluating CSF-CSF pressure propagation and blood-CSF propagation is not known. Thus, in this paper, the propagation properties of CSF were examined in detail in several healthy human subjects.

II. Material and Method

A. Correlation time mapping

The proposed technique works under the assumption that CSF is driven by pressure propagation from blood vessels and/or brain parenchyma and that CSF itself can be the media of such pressure propagation. The algorithm is based on the delay time of the flow velocity waveforms between a reference point and an arbitrary point in CSF space. First, 4D-PC MR velocimetry was used to take temporal change of flow velocities of CSF and blood along 3 spatial dimensions, x (Right-Left, RL), y (Anterior-Posterior, AP) and z (Superior-Inferior, SI) in a right-handed coordinate system during a cardiac cycle. Then the waveform of CSF or blood flow in a particular point in space was regarded as a reference point.

A waveform at an arbitrary point was assumed to have a delay from that at the reference point as pressure transmits with time. The delay time was calculated as the correlation time, or the amount of time shift, for the arbitrary waveform to

978-1-4244-7929-0/14/$26.00 ©2014 IEEE

have the highest correlation coefficient with the reference waveform as shown Fig. 1. The correlation coefficient was calculated with the following equations, which are different from those used in the pulsatility-based segmentation (PUBS) [10] in that the velocity waveform at the arbitrary location was shifted for a certain amount, d;

$$P_{x,y,d} = \frac{\sum_{k=1}^{N}\left(R_k - \bar{R}\right)\left(V_{x,y,k-d} - \bar{V}_{x,y}\right)}{\sqrt{\sum_{k=1}^{N}\left(R_k - \bar{R}\right)^2}\sqrt{\sum_{k=1}^{N}\left(V_{x,y,k-d} - \bar{V}_{x,y}\right)^2}} \quad (1)$$

$$(d = 0, 1, 2, \mathrm{L}, N-1)$$

where $P_{x,y,d}$ is the correlation coefficient with the delay time index d at an arbitrary location (x, y), R is the velocity of the reference waveform, $V_{x,y,k-d}$ is the velocity at the arbitrary spatial location and shifted for d points with respect to the original, k is the time index, and N is the total number of data points, and thus the number of images, within a cardiac cycle. The correlation time and the maximum correlation coefficient were obtained for all the voxels. The most imporatant variable derived from (1) is the correlation time, d_{max} giving the maximum value of $P_{x,y,d}$, because this tells the delay in the propagation of CSF. The maximum value of the correlation yielded by d_{max}, denoted as $P_{x,y,dmax}$, is also important since this represents the strength of the similarity between the reference and the target flows. Thus the maps of d_{max} and $P_{x,y,dmax}$ were mapped and visualized in color scales. Accuracy of (1) was validated by simulation.

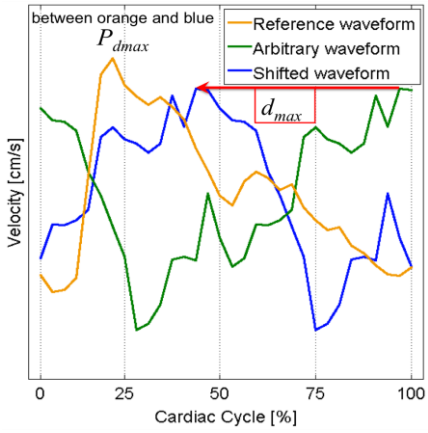

Fig. 1. Schematic diagram of the correlation time calculation. Orange line is the reference waveform of velocity at certain point, and green line is a waveform obtained at an arbitrary point in CSF space. The amount of time shift (d_{max}) to maximize the correlation (P_{dmax}) between the reference waveform and the waveform at an arbitrary point was defined as the correlation time.

B. Volunteer experiments

The volunteer studies were approved by the institutional review board (IRB). Appropriate informed consent was obtained for each volunteer. Image acquisitions were performed in 5 healthy volunteers, 5 male with mean age of 39, and 1 female patient with normal pressure hydrocephalus (NPH), age of 76. In this study, 4D-PC MR velocimetry in healthy volunteer experiments was performed in two velocity encoding (VENC), 5 and 100 cm/s, for obtaining accurate velocity of CSF and blood flow. The 4D-PC were obtained with the following conditions; flow encoding directions, RL, AP and IS; TR, 9.7-13.4 ms; TE, 5-13.7 ms; Flip angle (FA), 20°; Field of view (FOV), 30 × 30 cm2; Acquisition matrix, 320 × 320; VENC, 5, 20 (for the patient with NPH) and 100 cm/s; slice direction, sagittal. The imaging slab was at sagittal, and the image reconstruction was synchronized retrospectively by pulse from electrocardiograph (ECG). In healthy volunteer experiments, a location of arterial blood vessel was visualized by correlation coefficient mapping in set reference point at blood flow, then reference point was set at CSF space in nearby blood vessel based on obtained correlation coefficient map. In patient experiment, reference point was set as well based on visible blood flow in VENC 20. In the correlation mapping of CSF, average CSF velocity in the region of black rectangle was regarded as reference waveform. Both the maps were analyzed for the SI direction because the CSF flow dynamics was expected to be along mainly the to-and-fro motion in this direction. Color-coding of correlation time map used HSV color system because no delay and max delay are actually same time.

III. Result

Correlation time (a) and correlation coefficient (b) maps of the arterial blood flow of a healthy volunteer, in which reference point was set at basilar artery (yellow asterisk, *) are shown in Fig. 2. The images are showing high correlation coefficient area (R < 0.7). Orange and green circles in Fig. 2 show anterior cerebral artery (ACA) and vertebral artery, respectively. The Delay time map showed no delay, while the correlation coefficient map showed high correlation. Similar results were obtained for the other volunteers.

Typical results on a healthy volunteer are shown in Fig. 3. Results of the patient with NPH are shown in Fig. 4. In each figure, correlation time maps (a, c and e) and correlation coefficient maps (b, d and f) of CSF obtained with different reference regions (black rectangles in CSF near vertebral (a, b), basilar (c, d), and ACA (e, f)). In Fig. 3, images (a), (c) and (e) exhibited the transmitting flow induced by arterial vessels with relatively short delay. The delay map in image (a) was slightly different from that in images (c) and (e). Images (b), (d) and (f) showed relatively high correlation value within the vicinity of the reference point and in the aqueduct. In all healthy volunteers, correlation time and coefficient maps exhibited the propagation of CSF motion in the ventricular system with relatively short delay. The correlation coefficient was relatively low in the third ventricle.

On the other hand, the results for the NPH patient were different from those of healthy volunteer. In Fig. 4, the correlation time maps (a), (c) and (e) and the correlation coefficient maps (b), (d) and (f) were apparently different from the corresponding results of a typical healthy volunteer. The correlation times distributed in the wide region without remarkable feature as shown in (a), (c) and (e). The correlation coefficients shown in (b), (d) and (f) were clearly lower and more distributed than those of healthy volunteers.

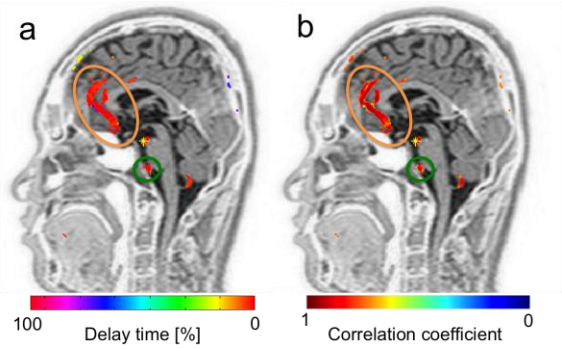

Fig. 2. Correlation time map (a) and correlation coefficient map (b) of arterial blood flow obtained with a reference point set at basilar artery (yellow asterisk, *). Orange and green circle indicate a location of anterior cerebral artery (ACA) and vertebral artery, respectively. The maps exhibited that the arterial blood flow propagates with no delay and with no waveform distortion.

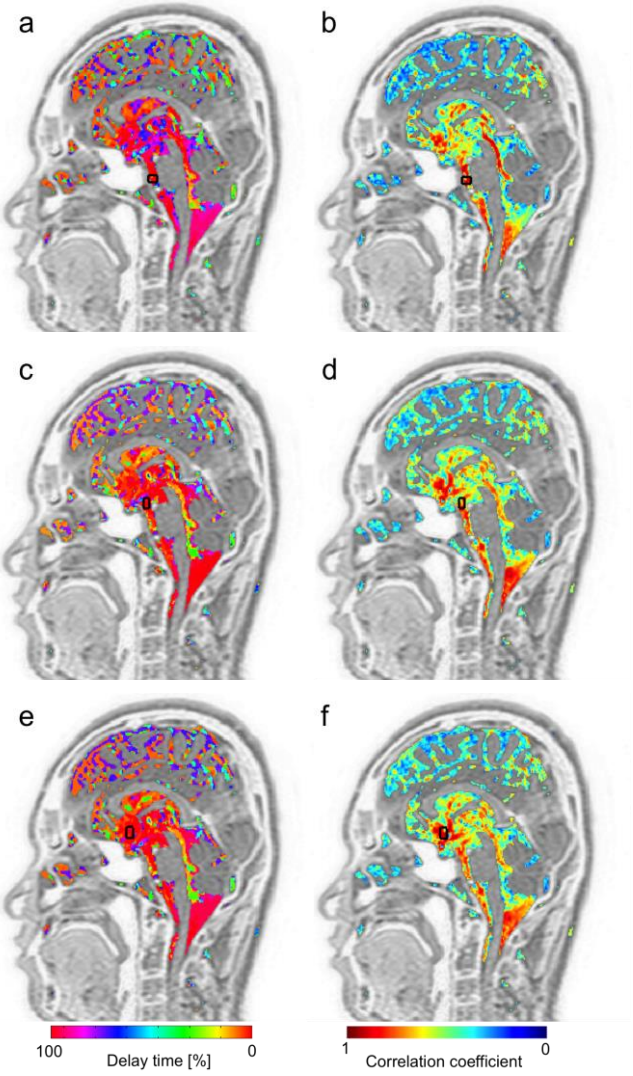

Fig. 3. Correlation time maps (a, c and e) and the correlation coefficient maps (b, d and f) of CSF at the midline slice position of a common healthy volunteer obtained with different reference regions in CSF near vertebral (a, b), basilar (c, d) and ACA (e, f), respectively. The time maps (a, c and e) and correlation maps (b, d and f) look like a little different distribution despite arterial blood flow propagates in the immediate delay, respectively.

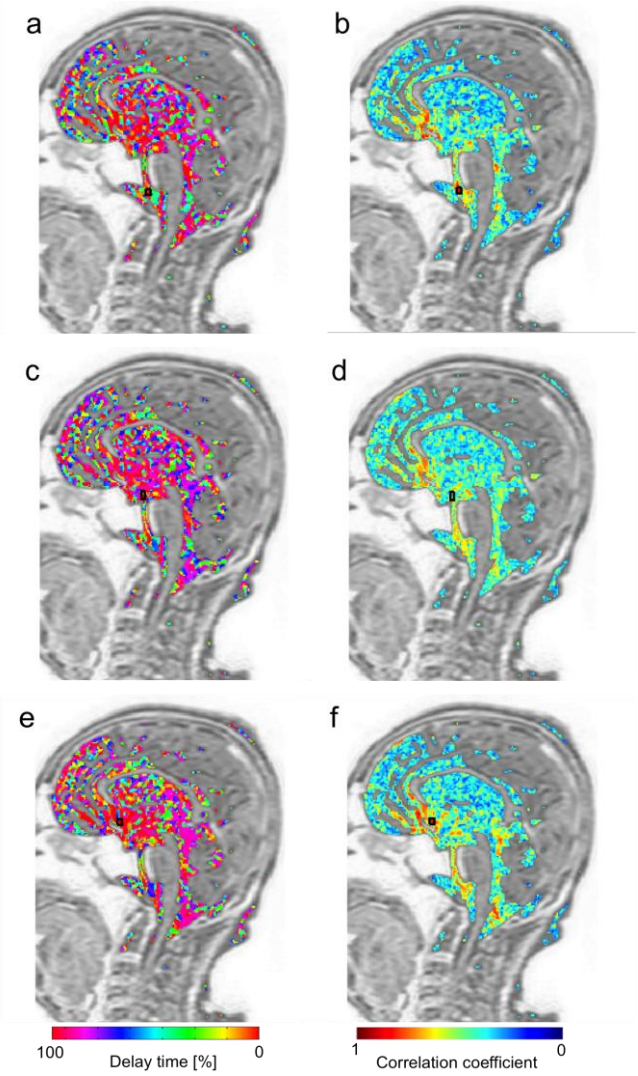

Fig. 4. Correlation time maps (a, c and e) and the correlation coefficient maps (b, d and f) of CSF at the midline slice position of the NPH patient obtained with different reference regions in CSF near vertebral (a, b), basilar (c, d) and ACA (e, f), respectively. The time maps (a, c and e) looked like to be reflecting CSF motion property. The correlation maps (b, d and f) showed clearly lower correlation distributions than that of healthy volunteers.

IV. Discussion

The correlation maps were evaluated for visualizing the CSF dynamics induced by pressure propagation from CSF and/or blood in 5 healthy volunteers and 1 NPH patient. The resultant maps seemed to be effective to "freeze" the complicated flow information obtained by the 4D-PC.

Correlation maps in Fig. 2 showed that the waveform of the arterial blood flow propagates with no delay and with high correlation. This implies that the arterial blood flow, which is regarded as non-compressible fluid, is propagates in the vessels with a relatively rigid wall. On the other hand, the correlation time maps in Fig. 3-4 exhibited the presence of propagation delay in CSF space. Since CSF itself is incompressible like blood, the results indicate that the CSF space is compressible. In other word, there seems to be compliance in the CSF space. The background causes of the compliance of the CSF space is not clear at this moment.

Possible explanation may be that compressibility of the vascular bed including the capillary and venous vessels, and/or of brain parenchyma. In either way, correlation time mapping has a potential to reflect such a fluid-mechanical property of the CSF space. This is also implicated in the experimental results that the different delay time distributions were observed with different reference points in the healthy volunteers. Correlation coefficient maps showed high correlation values in the regions near the reference points, and relatively low values in the regions far from the reference point. As the correlation coefficient map visualizes the similarity of spatiotemporal CSF velocity waveform pattern, the results mean that the degree of distortion of CSF velocity waveform increase with the distance from the reference point. In other words, the correlation time map and the correlation coefficient map reflect the compliance and the resistance properties in the CSF space.

In the results of the NPH patient, although correlation time maps exhibited propagating CSF motion with relatively short delay, its dynamics seemed to be more complicated than that of healthy volunteers, indicating that the NPH status changes the CSF circulation property. The correlation coefficient maps showed apparently low correlation distribution over the field of view. To date, the compliance of brain parenchyma in a patient with NPH is considered to be lower than that of the normal. Therefore, the relatively short delay and high correlation were expected because the fluid flow propagates more directly in the CSF space. However, apparently different result from this expectation appeared in the present study.

Also, there were slight individual difference among the healthy volunteers. The results suggest that the impact of blood vessels pulsation on CSF space may be different by circumstances such as a location of blood vessels. Thus, the interpretation of the results are not fully made and thus needs further studies. Nevertheless, the correlation mapping may characterize the CSF flow dynamics.

In conclusion, correlation time mapping as well as correlation coefficient mapping seemed to be useful for visualizing properties of CSF space such as compliance and resistance. The pressure propagation between the CSF parts at different locations as well as between blood flow and CSF were imaged in quantitative manner. The interpretation of the images for understanding the CSF driving force is not revealed yet. The mapping technique may be useful for classification of a disease such as hydrocephalus.

The interpretation of the data has to be examined further based on phantom experiments and numerical simulations in order to apply the present technique to the investigation of the CSF driving force origin. Criterion related to the placement of the reference point is important. The applicability of the technique in clinical situations has to be discussed also.

REFERENCES

[1] Henry-Feugeas MC, idy-Peretti I, Baledent O, Poncelet-Didon A, Zannoli G, Bittoun J, Schouman-Claeys E. Origin of subarachnoid cerebrospinal fluid pulsations: a phase-contrast MR analysis. Magn Reson Imag 2000;18(4):387–95.

[2] Yamada S, Miyazaki M, Kanazawa H, Higashi M, Morohoshi Y, Bluml S, McComb JG. Visualization of cerebrospinal fluid movement with spin labeling at MR imaging: preliminary results in normal and pathophysiologic conditions. Radiology 2008 Nov;249(2):644-52. doi: 10.1148/radiol.2492071985.

[3] Matsumae M, Hirayama A, Atsumi H, Yatsushiro S, Kurda K. Velocity and pressure gradients of cerebrospinal fluid assessed with magnetic resonance imaging. J Neurosurg. 2014 Jan;120(1):218-27. doi: 10.3171/2013.7.JNS121859. Epub 2013 Aug 9.

[4] Bunck AC, Kröger JR, Jüttner A, Brentrup A, Fiedler B, Schaarschmidt F, Crelier GR, Schwindt W, Heindel W, Niederstadt T, Maintz D. Magnetic resonance 4D flow characteristics of cerebrospinal fluid at the craniocervical junction and the cervical spinal canal. Eur Radiol. 2011 Aug;21(8):1788-96. doi: 10.1007/s00330-011-2105-7. Epub 2011 Mar 15.

[5] Bunck AC, Kroeger JR, Juettner A, Brentrup A, Fiedler B, Crelier GR, Martin BA, Heindel W, Maintz D, Schwindt W, Niederstadt T. Magnetic resonance 4D flow analysis of cerebrospinal fluid dynamics in Chiari I malformation with and without syringomyelia. Eur Radiol. 2012 Sep;22(9):1860-70. doi: 10.1007/s00330-012-2457-7. Epub 2012 May 9.

[6] Hirayama A, Yatsushiro S, Abdulla A, Atsumi H, Kuroda K, Matsumae M. Visualization of pulsatile cerebrospinal fluid motion around membrane-like structures by using four-dimensional phase-contrast (4D-PC) velocity mapping. J Magn Reson Med 2014 (submitted)

[7] Yatsushiro S, Hirayama A, Atsumi H, Matsumae M, Kuroda K. Correlation time mapping based on magnetic resonance velocimetry: preliminary results on cerebrospinal fluid flow. BMEiCON 2013: 26-27.

[8] Yatsushiro S, Hirayama A, Matsumae M, Atsumi H, Kuroda K. Visualization of cerebrospinal fluid propagation based on correlation time mapping. MJJIS 2013: 24.

[9] Lo EH, Rogowska J, Bogorodzki P, Trocha M, Matsumoto K, Saffran B, Wolf GL. Temporal correlation analysis of penumbral dynamics in focal cerebral ischemia. J Cereb Blood Flow Metab. 1996 Jan;16(1):60-8.

[10] Alperin N, Lee SH. PUBS: pulsatility-based segmentation of lumens conducting non-steady flow. Magn Reson Med 2003; 49:934–944.

[11] Abdullah A, Hirayama A, Yatsushiro S, Matsumae M, Kuroda K. Cerebrospinal fluid image segmentation using spatial fuzzy clustering method with improved evolutionary Expectation Maximization. Conf Proc IEEE Eng Med Biol Soc. 2013;2013:3359-62. doi: 10.1109/EMBC.2013.6610261.